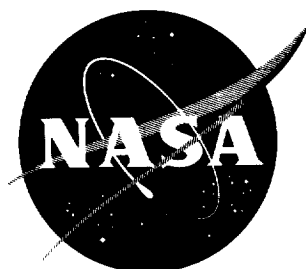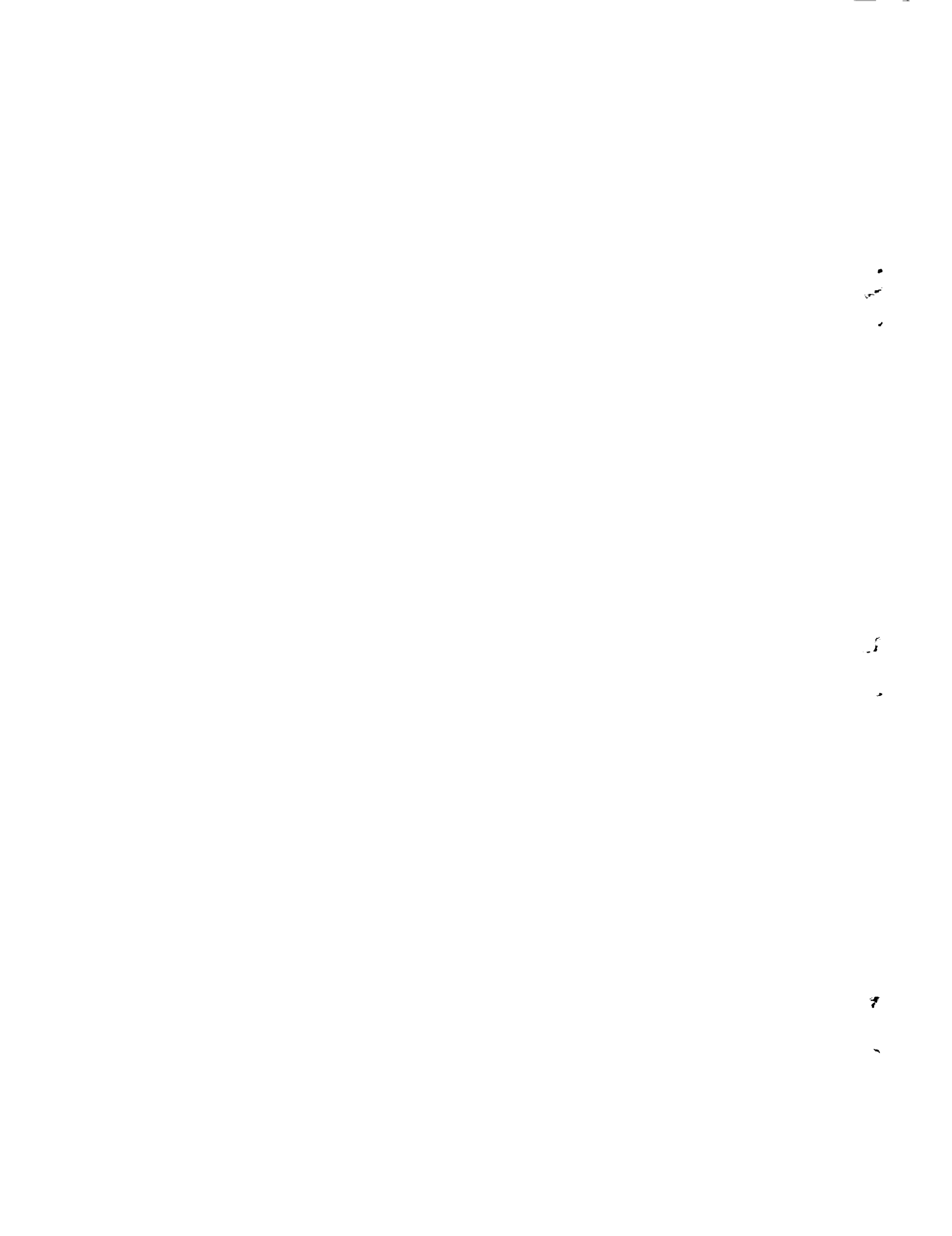NASA TN D-916

TECHNICAL NOTE

D-916

AERODYNAMIC CHARACTERISTICS AT A MACH NUMBER OF 3.10

OF SEVERAL FOURTH-STAGE SHAPES OF

THE SCOUT RESEARCH VEHICLE

By Byron M. Jaquet

Langley Research Center
Langley Field, Va.

NATIONAL AERONAUTICS AND SPACE ADMINISTRATION

WASHINGTON   June 1961

T

NATIONAL AERONAUTICS AND SPACE ADMINISTRATION

TECHNICAL NOTE D-916

AERODYNAMIC CHARACTERISTICS AT A MACH NUMBER OF 3.10

OF SEVERAL FOURTH-STAGE SHAPES OF

THE SCOUT RESEARCH VEHICLE

By Byron M. Jaquet

SUMMARY

A wind-tunnel investigation was made at a Mach number of 3.10 (Reynolds number per foot of 16.3×10^6 to 16.9×10^6) to determine the aerodynamic characteristics of various modifications of the payload section of the fourth stage of the Scout research vehicle. It was found that, for the combination of stages 3 and 4, increasing the size of the nose of the basic Scout to provide a cylindrical section of the same diameter as the third stage increased the normal-force slope by about 30 percent, the axial force by about 39 percent, and moved the center of pressure forward by about one fourth-stage base diameter. By reducing the diameter of the cylinder, at about one nose length behind the base of the enlarged nose frustum, to that of the basic Scout and thereafter retaining the shape of the basic Scout, the center of pressure was moved rearward by about one-half fourth-stage base diameter at the expense of an additional 19-percent increase in axial force. A spike-hemisphere configuration had the largest forces and moments and the most forward center-of-pressure location of the configurations considered.

Except for the axial force and pitching-moment slope, the experimental trends or magnitudes could not be estimated with the desired accuracy by Newtonian or slender body theory.

INTRODUCTION

In order to accommodate various payloads on the Scout research vehicle, several fourth-stage configurations have been suggested. Since a knowledge of the aerodynamic forces and moments is necessary in order to determine the structural requirements and the dynamic characteristics of the vehicle, a brief wind-tunnel investigation of a group of configurations was undertaken at the Langley Research Center at the request of the Scout Project Office. The investigation was concerned with the measurement at a Mach number of 3.10, through a small angle-of-attack range, of normal force,

2

axial force, and pitching moment of several fourth-stage configurations,
with and without the third stage. The Reynolds number per foot was about
16.3×10^6 to 16.9×10^6 for the tests. The experimental data were also
compared with Newtonian and slender body theory.

SYMBOLS

Coefficients are referred to the body system of axes shown in fig-
ure 1 with the moment center in all cases being at the base of the fourth
stage. (See fig. 2.) All coefficients are based on the area and diameter
of the base of the fourth stage.

C_A axial-force coefficient, $\dfrac{\text{Axial force}}{qA}$

$C_{A,b}$ base axial-force coefficient, $\dfrac{\text{Base axial force}}{qA}$

C_N normal-force coefficient, $\dfrac{\text{Normal force}}{qA}$

C_m pitching-moment coefficient, $\dfrac{\text{Pitching moment}}{qAD}$

A area of base of fourth stage

A_F area of base of first frustum of fourth stage

D diameter of base of fourth stage

q dynamic pressure

α angle of attack

$C_{N_\alpha} = \dfrac{\partial C_N}{\partial \alpha}$, per deg

$C_{m_\alpha} = \dfrac{\partial C_m}{\partial \alpha}$, per deg

MODELS AND EQUIPMENT

Drawings of the 0.0536-scale models of the fourth and third stages
of the Scout are shown in figure 2. The models were machined from

duralumin with the exception of the spike of model 5, which was turned from a steel rod. A shroud was used to prevent air from striking the balance when only the fourth stage was tested. As shown in figure 2, the shroud extended into but did not touch the base of the fourth stage nor did it touch the balance.

The models were tested in a Mach number 3.10 blowdown jet at the Langley Research Center. The test section of the jet measured approximately 12 inches in width by $12\frac{1}{2}$ inches in height.

An electrical strain-gage balance was attached to a sting, the models being attached to the balance. The sting was hydraulically driven through an angle-of-attack range in increments of about $1\frac{3}{4}^{\circ}$.

TESTS AND CORRECTIONS

The tests consisted of the measurement of normal force, axial force, and pitching moment at 0° sideslip through an angle-of-attack range of about $\pm 3\frac{1}{2}^{\circ}$ for each of the fourth-stage models of figure 2 with and without the third stage. All tests were made at a stagnation temperature of about 100° F and at stagnation pressures from 100 to 104 pounds per square inch gage which correspond to a Reynolds number per foot of about 16.3×10^{6} to 16.9×10^{6}. Base pressures were measured within the models and the axial forces were adjusted to correspond to a base pressure equivalent to the free-stream static pressure. The angle of attack was corrected for the deflection of the sting and balance under load.

ACCURACY

The data presented herein are believed to be accurate to within the following limits:

α, deg . . . . ± 0.10
Mach number . . . . ± 0.015
C_A, C_N . . . . ± 0.010
C_m . . . . ± 0.014

RESULTS AND DISCUSSION

Presentation of Results

The data of the present investigation are arranged to show primarily three effects. First, it was desired to show the effect of increasing the size of the nose of stage 4 (basic Scout nose, fig. 2, model 1) until the frustum at the base of stage 4 was eliminated (model 3). Then it was desired to determine whether a rearward center-of-pressure shift could be accomplished by notching model 3 to form model 4. The hemispherical nose of model 5 was selected since it was expected on the basis of Newtonian theory to have a lower value of C_{N_α} than the nose of model 4. In order to reduce the large axial force associated with a hemisphere, the spike was added to model 5. On the basis of reference 1, it might be expected that the effects of the spike on C_{N_α} and C_{m_α} would be significant. Also of interest was the effect of the addition of the third stage to each of the fourth-stage models.

The data of the present investigation are summarized in figure 3 in which are presented normal-force and pitching-moment slopes, axial-force coefficient, and center-of-pressure location at an angle of attack of $0°$. These data were determined from the data of figures 4 to 7 with the slopes measured over the maximum angle-of-attack range since it was felt that this procedure would give the most accurate values. The curves, in general, were linear over the angle-of-attack range investigated. The only exception was the curves for model 5 which were nonlinear over the angle-of-attack range, and the slopes were read, therefore, over a range of about $\pm 1\frac{3}{4}°$. Base axial-force coefficients are presented in figure 8.

Effect of Increase of Fourth-Stage Nose Size

Increasing the length and diameter of the nose in proportion to the fixed cone angle, the cylinder length, and diameter (the cylinder fineness ratio changes only slightly) and decreasing the size of the last frustum in changing from model 1 to model 3 (fig. 3) caused large increases in the normal-force and pitching-moment slopes, in axial force, and a forward shift in the center of pressure. The increase in axial force is probably directly associated with the increase in nose frustum size whereas the increase in normal-force slope is attributable to the increase in nose-frustum size and the carryover of the load from the nose frustum to the cylindrical sections. This load carryover would be expected to be greatest for the model with the largest diameter nose. The increase in pitching-moment slopes results from the increase in normal force due to the increase in nose-frustum size and the accompanying forward shift in center of pressure.

The addition of the third stage to each of the models caused an increase in normal-force slope and axial force and a rearward shift in the center of pressure as would be expected. Since the magnitude of the changes are least for model 3, it would appear that there is some load carryover from the last frustum of the fourth stage to the forward part of the cylinder of the third stage which, of course, decreases as the last frustum size is decreased. The aerodynamic parameters and center-of-pressure location for model 3 are in agreement with those reported in reference 1 for similar configurations.

The aerodynamic characteristics of the three models were determined from Newtonian considerations (ref. 3) and slender body theory (ref. 4). Estimates were made for stage 4 and in some cases, for stages 4 plus stage 3. These data are presented in figure 3 as are the Newtonian coefficients for the nose sections only of models 1 to 3. The trend of the experimental data with increasing nose size is predicted reasonably well by Newtonian theory when only the nose sections are considered. The Newtonian magnitudes however are considerably lower. When the contribution of the frustum at the base of stage 4 is considered, the Newtonian value for normal-force slope for model 1 is almost equal to the experimental value. However, as the size of the nose frustum is increased, the Newtonian contribution of the last frustum decreases to such an extent that the normal-force slope for model 3 is slightly lower than that for model 1 and is, as a result, considerably lower than the experimental value for model 3. The Newtonian method of reference 3 gives zero for the normal-force slope for the cylinder and no consideration has been given to flow-separation effects. It has been shown in reference 5 that boundary-layer separation can appreciably influence the aerodynamics of such configurations as those investigated herein and that, if a knowledge of the boundary-layer conditions exists from flow photographs, the body shape can be modified to obtain more accurate estimates of the aerodynamic parameters. The viewing window of the test section used in the present investigation permitted viewing only the part of the models extending rearward from the last frustum of the fourth stage and thus adequate flow photographs, from which modified shapes could be determined, could not be obtained. Slender body theory predicts the same value of normal-force slope for models 1, 2, and 3 and is in agreement with the experimental value only for model 1. The variation of pitching-moment slope with increasing nose size is predicted reasonably well in magnitude and trend only by slender body theory. The axial-force coefficient is predicted with good accuracy by Newtonian theory but the forward center-of-pressure shift with increasing nose size is considerably overestimated by both methods. (See fig. 3(b).)

In general, when stages 4 and 3 are considered, in order to increase the payload section size from the basic Scout (model 1) to that which has a cylindrical section (model 3) increases in normal force of about

30 percent, in axial force of about 39 percent, and a forward shift of center of pressure of about one fourth-stage base diameter were obtained.

Effect of Other Modifications

In order to form model 4, the diameter of the cylindrical section of model 3 was abruptly reduced at about one nose length rearward of the nose frustum base. The shape of model 1 was retained rearward of this point. These changes produced a decrease in both normal-force and pitching-moment slopes, an increase of about 19 percent in axial force, and about a 1/2-diameter rearward shift in the center of pressure. (See fig. 3.) The normal-force and pitching-moment slopes predicted by Newtonian and slender body theories are considerably lower than the experimental values and the center-of-pressure shift is considerably overestimated. In estimating the axial-force coefficient, the axial force due to the notch was determined from two-dimensional base pressures on a wedge (ref. 6) with the appropriate area considerations. This value was added to the Newtonian value and from figure 3(b) it can be seen that the axial-force coefficient is predicted reasonably well.

The spiked hemisphere nose configuration (model 5) was selected on the basis of the study of reference 7, the length being selected for minimum drag at zero angle of attack at a Mach number of 6.8. Model 5 has considerably higher values of the aerodynamic parameters than all other configurations and has a more forward center-of-pressure location than model 4. (Although the model was not tested with the spike removed, some information regarding the spike effects can be obtained by making a comparison of the present data with that in reference 8 for a hemisphere-cylinder tested at a Mach number of 2.98.)

The axial-force coefficient for model 5 increases rapidly with an increase in angle of attack whereas for all other models the axial force is essentially invariant with angle of attack. (See figs. 6 and 7.) This trend was also noted in references 9 and 1 at Mach numbers of 2.5 and 2.91, respectively. Estimation of the aerodynamic parameters of model 5 was attempted by considering an equivalent cone of $8°$ half angle and using Newtonian theory. This method considerably underestimated the normal-force and pitching-moment slopes. (See fig. 3.) The axial-force coefficient, accounting for the notch, was 0.10, which is very low compared with the experimental value. It would appear that flow separation may occur on the spike rearward of the shoulder and that the equivalent cone would have a larger angle. (The effects of spike length on flow separation along the spike are discussed in references 1 and 7 to 9.) From the experimental axial-force coefficient an equivalent cone of $33.5°$ half angle is obtained from Newtonian theory. (See ref. 3.) This cone angle, however, results in a much lower value of normal-force slope because by Newtonian theory C_{N_α} decreases with an increase in cone angle.

CONCLUSIONS

A wind-tunnel investigation of various modifications to the payload section of the fourth stage of the Scout research vehicle has indicated the following conclusions:

1. For the combination of the third and fourth stages, increasing the size of the nose frustum of the nose of the basic Scout to provide a cylindrical section of the same diameter as the third stage increased the normal-force slope by about 30 percent, the axial force by about 39 percent, and moved the center of pressure forward by about one fourth-stage diameter.

2. By reducing the diameter of the cylinder of the largest model, at about one nose length behind the base of the nose frustum, to that of the basic Scout and thereafter retaining the shape of the basic Scout the center-of-pressure movement was reduced by about one-half but the axial force was increased by an additional 19 percent.

3. A spike-hemisphere configuration had the largest forces and moments and the most forward center-of-pressure location of the configurations considered.

4. Except for the axial force and pitching-moment slope, the experimental trends or magnitudes could not be estimated with the desired accuracy by Newtonian or slender body theory.

Langley Research Center,
    National Aeronautics and Space Administration,
        Langley Field, Va., April 24, 1961.

REFERENCES

1. Harman, Richard W., and Boatright, William B.: Investigation of the Aerodynamic Characteristics of a Reentry Capsule With Various Nose Shapes at a Mach Number of 2.91, Including Studies of Nose Spikes as a Means of Control. NASA TM X-426, 1961.

2. Kingsley, R. J., and Chadwick, G. A.: Results of Static Force and Moment Parametric Study Conducted in the JPL 20 Inch Supersonic Wind Tunnel - JPL 20-342 and JPL 20-351. Tech. Memo. RAD-9-TM-59-48 (Contract AF04(647)-305) AVCO Res. and Advanced Dev. Div., Aug. 14, 1959.

3. Fisher, Lewis R.: Equations and Charts for Determining the Hypersonic Stability Derivatives of Combinations of Cone Frustrums Computed by Newtonian Impact Theory. NASA TN D-149, 1959.

4. Tobak, Murray, and Wehrend, William R.: Stability Derivatives of Cones at Supersonic Speeds. NACA TN 3788, 1956.

5. Dennis, David H.: The Effects of Boundary-Layer Separation Over Bodies of Revolution With Conical Tail Flares. NACA RM A57I30, 1957.

6. Love, Eugene S.: Base Pressure at Supersonic Speeds on Two-Dimensional Airfoils and on Bodies of Revolution With and Without Fins Having Turbulent Boundary Layers. NACA TN 3819, 1957. (Supersedes NACA RM L53C02.)

7. Crawford, Davis H.: Investigation of the Flow Over a Spiked-Nose Hemisphere-Cylinder at a Mach Number of 6.8. NASA TN D-118, 1959.

8. Smith, Fred M.: A Wind-Tunnel Investigation of Effects of Nose Bluntness, Face Shape, and Afterbody Length on the Aerodynamic Characteristics of Bodies of Revolution at Mach Numbers of 2.37, 2.98, and 3.90. NASA TM X-230, 1960.

9. Rubin, Eugene S.: Resumé of Naval Supersonic Laboratory Infrared Effort Leading to a Possible Solution to the "Hot-Window Problem." Tech. Rep. 155 (Contract AF33(616)-2107) Naval Supersonic Lab., M.I.T., 1955.
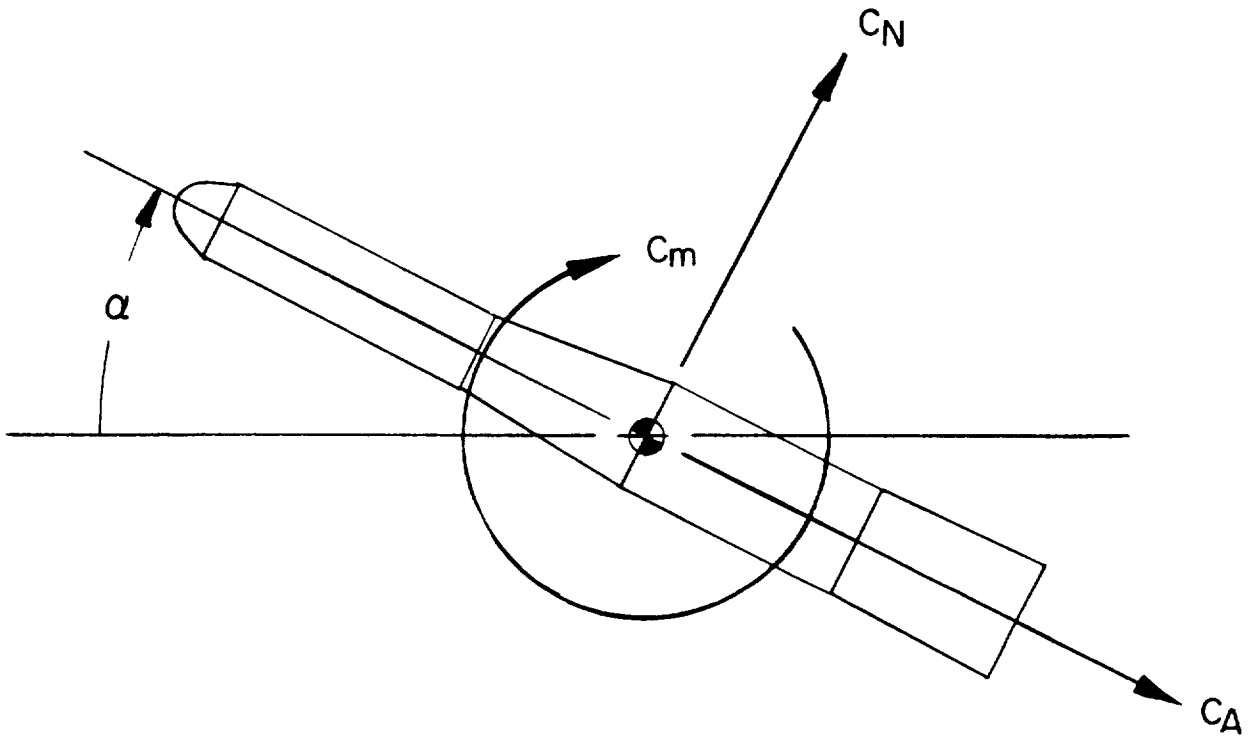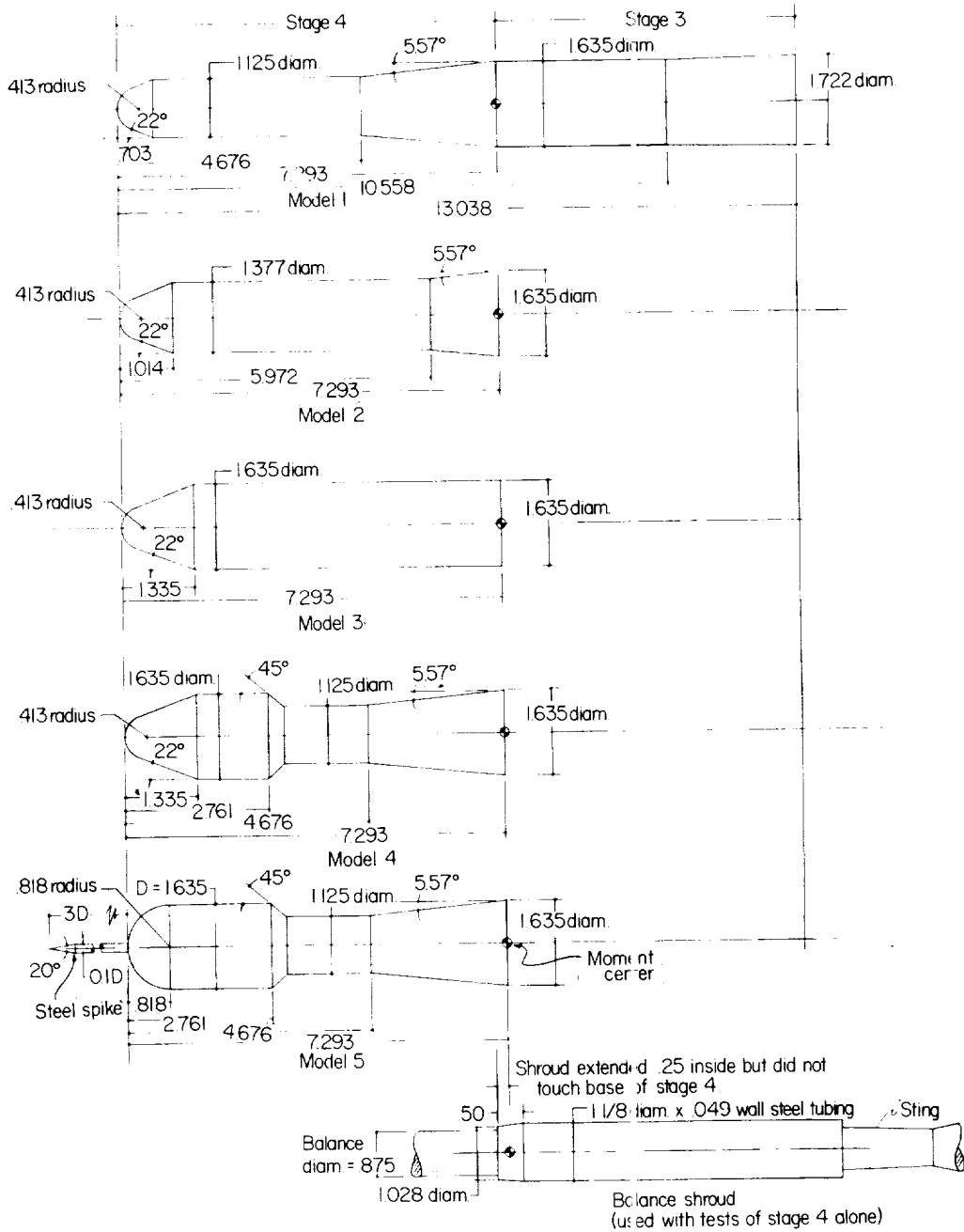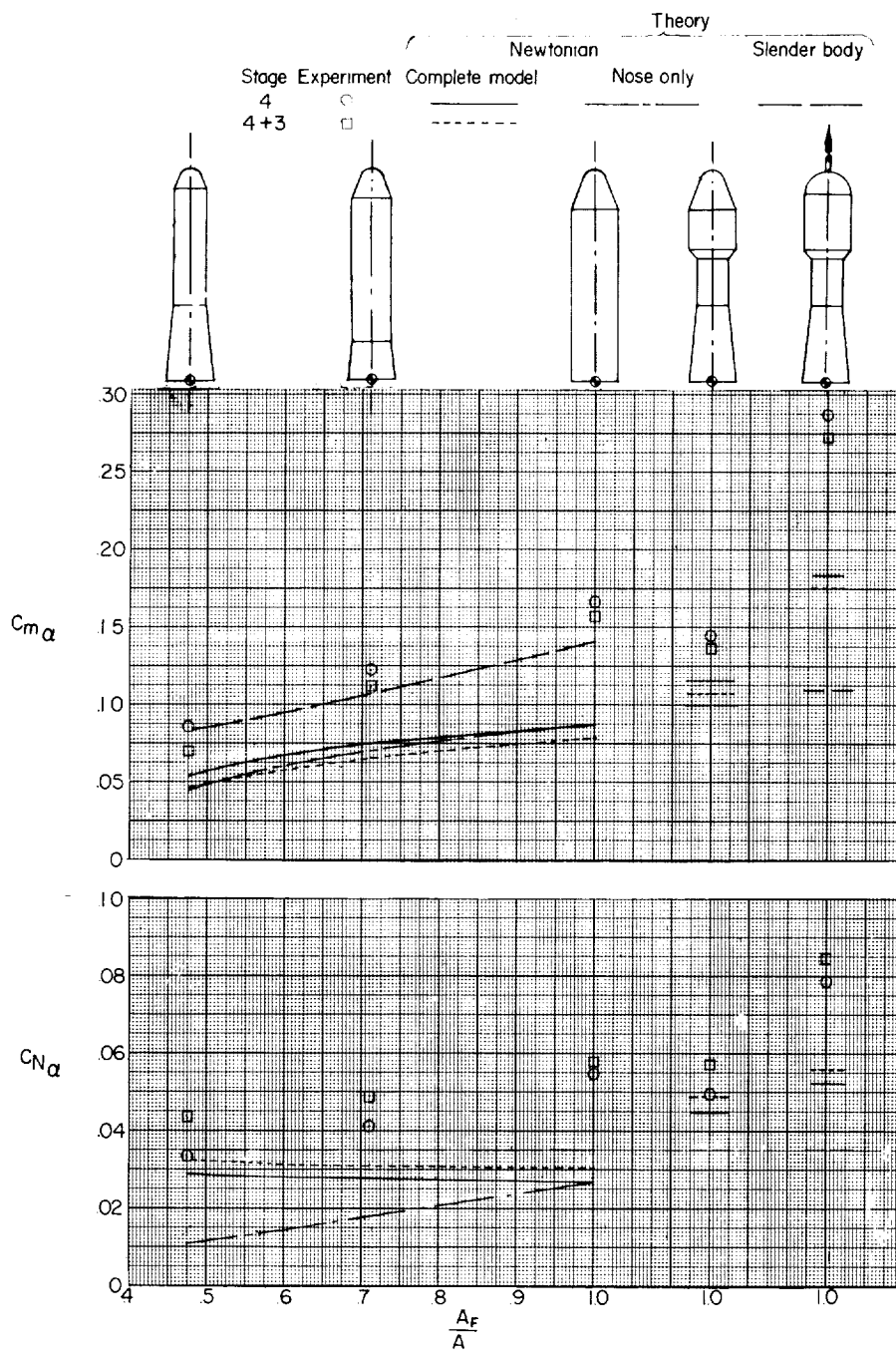
L
1
5
7
8

Figure 1.- Body system of axes with positive coefficients and angle of
attack shown.

Figure 2.- General arrangement of 0.05360-scale models of Scout research vehicle. All dimensions are in inches unless otherwise noted. All stage 4 models interchangeable with stage 3.

(a) Variation of pitching-moment and normal-force slopes with size of base of first frustum of stage 4.

Figure 3.- Summary of aerodynamic characteristics of fourth- and third-stage Scout configurations.
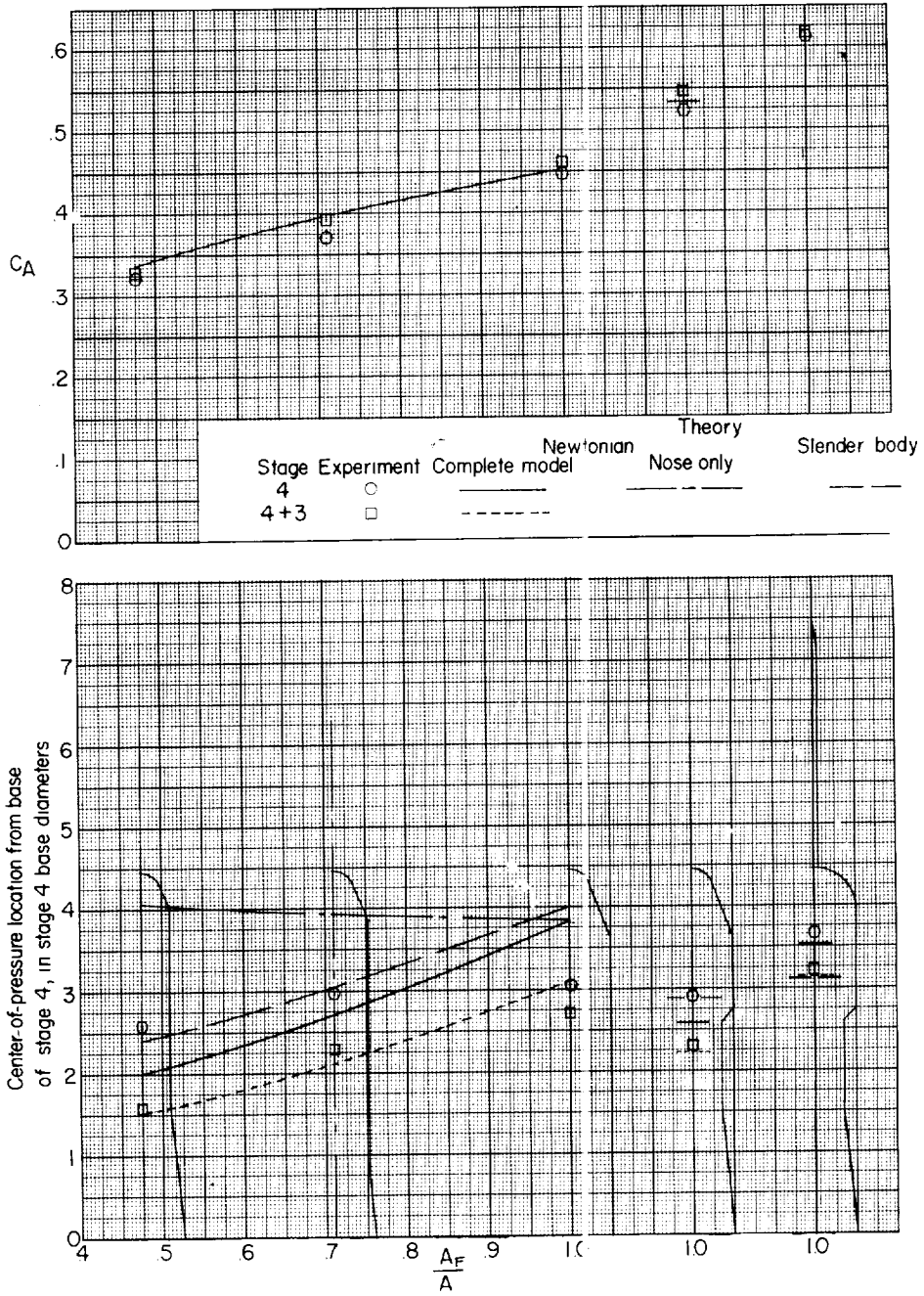
(b) Variation of axial-force coefficient and center-of-pressure
    location with size of base of first frustum of stage 4.
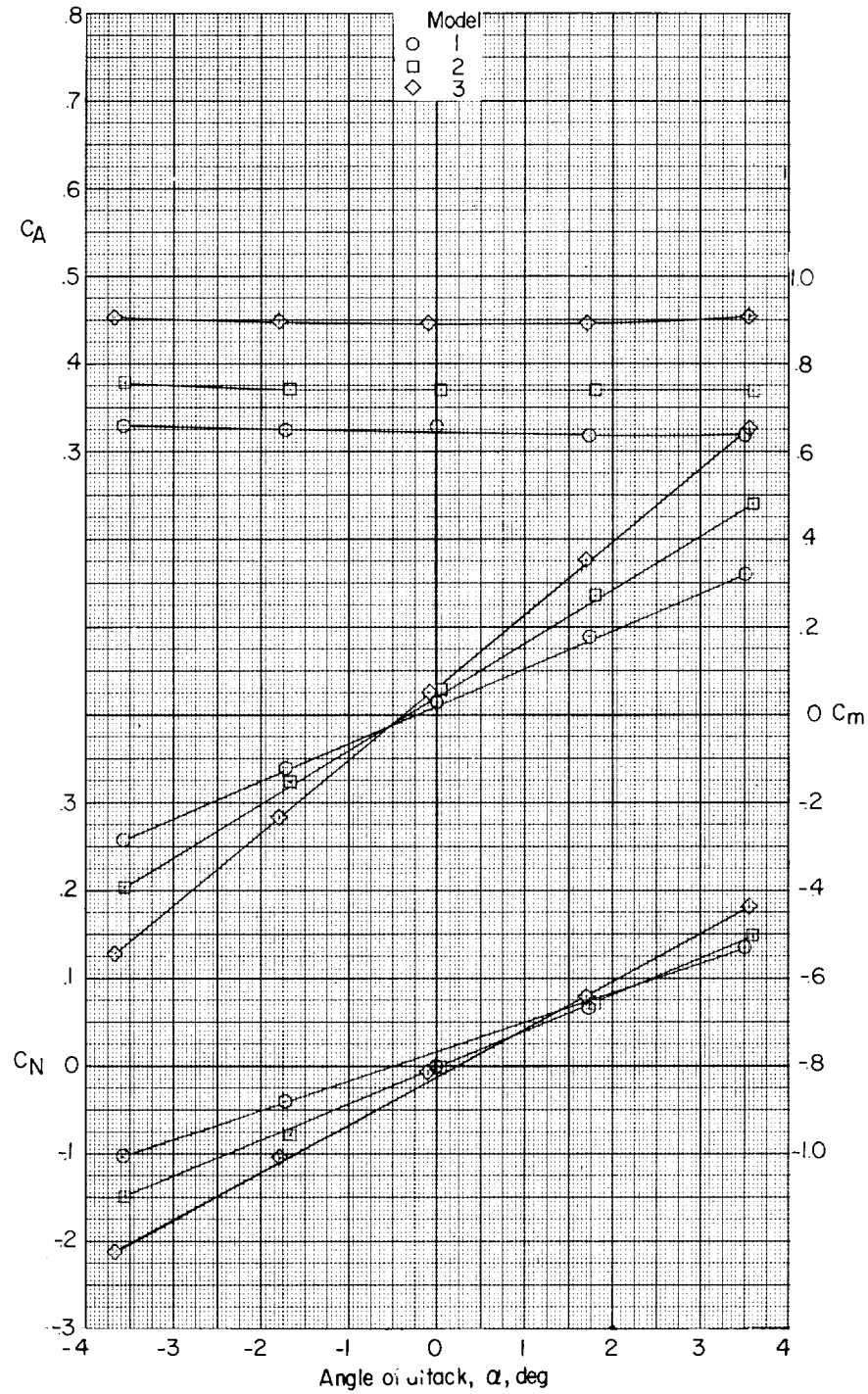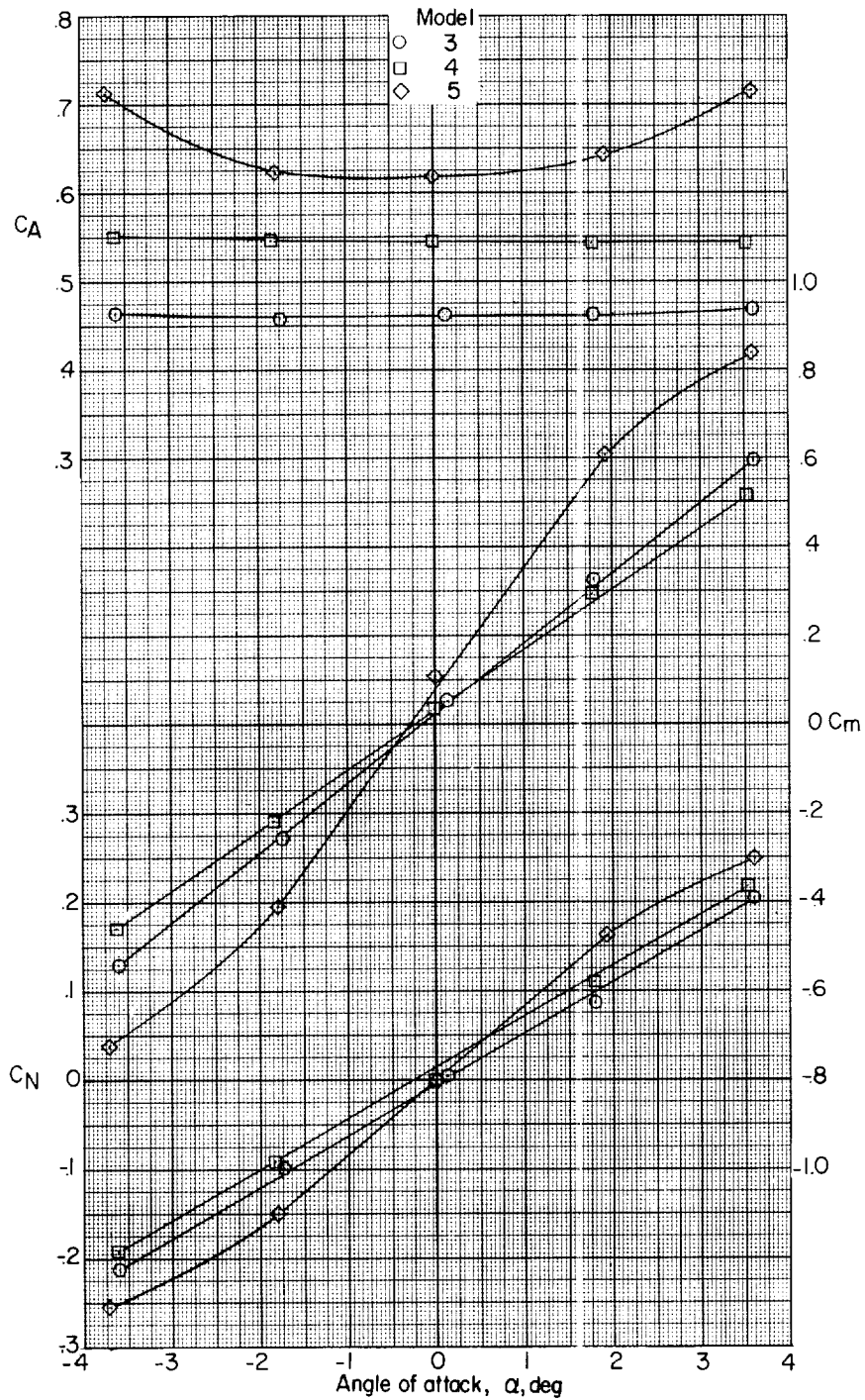
Figure 3.- Concluded.

L-1578

Figure 4.- Variation of C_A, C_m, and C_N with angle of attack for
models 1, 2, and 3. Fourth-stage configurations.

Figure 6.- Variation of C_A, C_m, and C_N with angle of attack for
models 3, 4, and 5. Fourth-stage configurations.

16

Figure 7.- Variation of C_A, C_m, and C_N with angle of attack for models 3, 4, and 5. Third- and fourth-stage configurations.
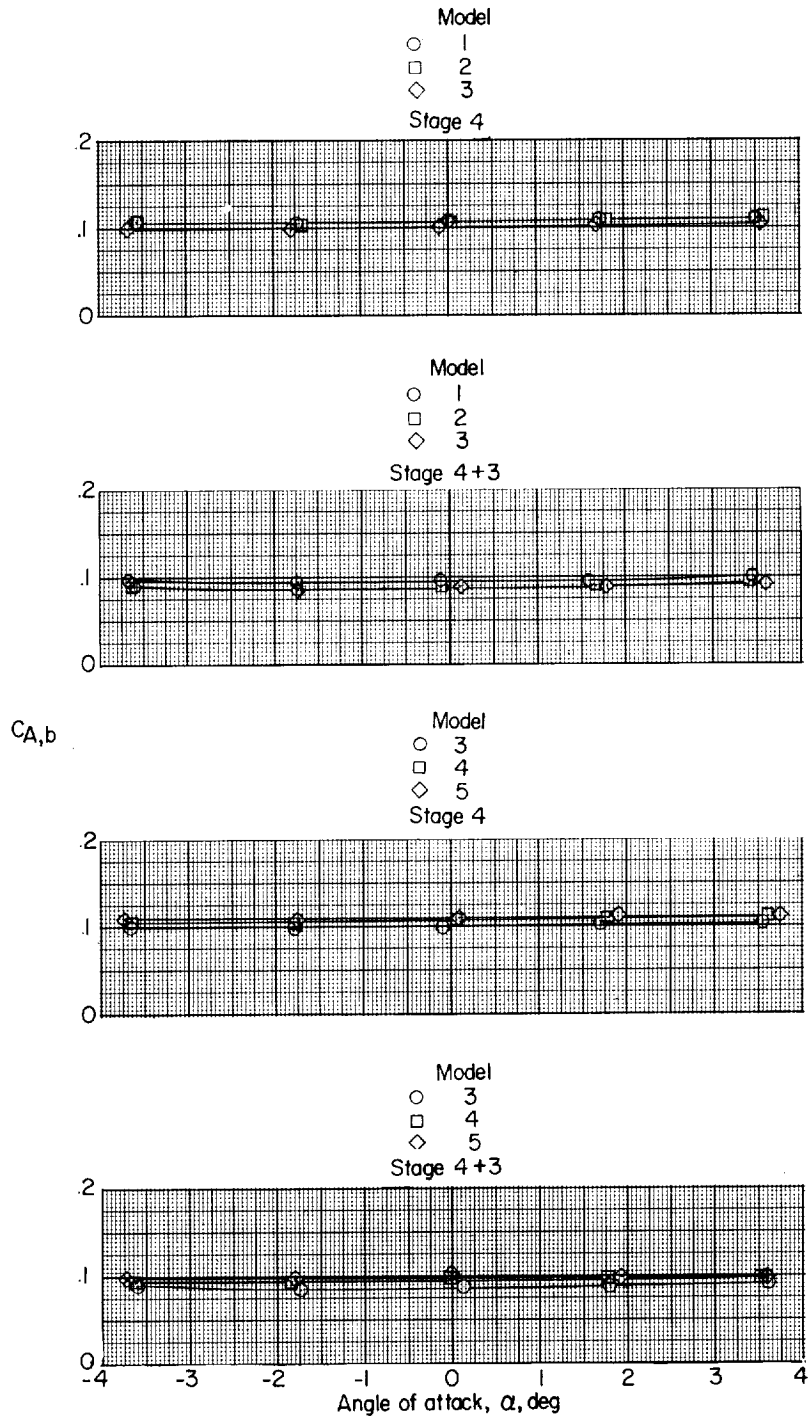
L-1578

Figure 8.- Variation of $C_{A,b}$ with angle of attack for configurations tested.